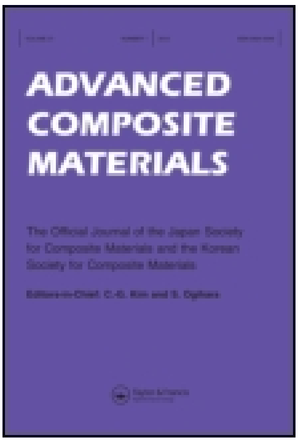

Advanced Composite Materials
Publication details, including instructions for authors and subscription information:
http://www.tandfonline.com/loi/tacm20

Mode II interlaminar properties under static and fatigue loadings for CF/epoxy laminates with different fiber-surface treatment

M. Hojo , S. Matsuda , S. Ochiai , N. Tsujioka , Y. Nakanishi , Z. Maekawa & A. Murakami

Version of record first published: 02 Apr 2012.

Adv. Composite Mater., Vol. 10, No. 2,3, pp. 237–246 (2001)

Mode II interlaminar properties under static and fatigue loadings for CF/epoxy laminates with different fiber-surface treatment

M. HOJO [1], S. MATSUDA [2], S. OCHIAI [1], N. TSUJIOKA [3], Y. NAKANISHI [1], Z. MAEKAWA [4] and A. MURAKAMI [2]

[1] *Mesoscopic Materials Research Centre, Graduate School of Engineering, Kyoto University, Kyoto 606-8501, Japan*
[2] *Department of Chemical Engineering, Himeji Institute of Technology, Himeji 671-2201, Japan*
[3] *Asahi Chemical Co. Ltd., Moriyama 424-0002, Japan*
[4] *Division of Advanced Fibro-Science, Kyoto Institute of Technology, Kyoto 606-8585, Japan*

Abstract—The effect of fiber-surface treatment on delamination fatigue under mode II loading was investigated for unidirectional CF/epoxy laminates. Two types of laminates were made from surface-treated or surface-non-treated carbon fiber, and a common epoxy matrix. Tests were carried out using end notched flexure (ENF) specimens. Stabilized mode II static tests showed that the fracture toughness of the surface-treated CFRP was 30% higher than that of non-treated CFRP. Fatigue crack growth resistance of the surface-treated CFRP was higher than that of non-treated CFRP at higher crack growth rate. However, the effect of fiber surface treatment was negligible near the threshold region. At higher growth rate, interfacial fracture occurred prior to the matrix fracture near the crack tip for the non-treated CFRP. Then, the fracture mechanism was controlled by the interfacial fracture. On the other hand, the resin fracture with plastic deformation occurred prior to the interfacial fracture near the crack tip for the surface-treated CFRP. Then, the fracture mechanism was controlled by the resin fracture. Near the threshold region, the ratio of the resin fracture was rather large without respect to the fiber-surface treatment. The main fracture mechanisms near the threshold region were only controlled by the matrix resin. This fact was well correlated to the fact that the threshold value was insensitive to the fiber-surface treatment.

Keywords: CFRP; delamination; Mode II; surface-treatment; fracture taghness; fatique threshold.

1. INTRODUCTION

The most common damage mechanism in laminated composite structures is delamination. Although this topic has been investigated for more than twenty years, most of these approaches are rather macroscopic, and the role of mesoscopic components of composite laminates such as resin and interface has not been understood in detail. Several researches have already been carried out to investigate the effect of the surface treatment of fiber on the macroscopic fracture behavior [1, 2]. However, these research works are based on laminates produced in laboratories. Thus, it is rather difficult to clarify only the effect of the fiber surface treatment because other mesoscopic factors such as the geometrical arrangement of fiber also change simultaneously for laminates made in-house.

We have launched a series of research works to investigate the effect of surface treatment on the composite properties by producing fibers and prepregs at an industrial manufacturing plant. The influences on the interfacial strength and the static mode I interlaminar properties have already been reported [3, 4].

In the present study, the effects of fiber surface treatment on the interlaminar fracture toughness and the delamination fatigue crack growth behavior under mode II loading were investigated for unidirectional CF/epoxy laminates. The mechanism of the effect of the fiber-surface treatment was discussed on the bases of fracture mechanical consideration and microscopic observation.

2. EXPERIMENTAL PROCEDURE

2.1. Material and specimen

The carbon fiber used in this study was PAN based AT400 (Asashi Chemical, strength = 3.9 GPa, modulus = 240 GPa). The surface treatment of fiber was carried out by the anodic oxidation method [5] in 8% aqueous nitric acid using a current of electricity of 27.6 C/m^2. The surface oxygen content on the carbon fiber surface was 0.15 by X-ray photoelectron spectroscopy (XPS), and the acid function was 12×10^{-6} eq/m^2 by neutralization titration. Non-treated fiber was also used for comparison. Two types of laminates were made from surface-treated or surface-non-treated carbon fiber and a common bisphenol A type epoxy matrix (modified epoxy resin with lower cross-linking density and higher toughness). These are designated as surface-treated CFRP and non-treated CFRP.

Unidirectional laminates, $(0)_{26}$ ($V_f = 54\%$), of the thickness of 3 mm were molded in an autoclave. The manufacturing process of fiber and prepregs was fully controlled to avoid any influences such as irregularity coming from handmade prepregs, etc. This controlled process is essential because interlaminar fracture properties are very sensitive to the distribution of fibers and matrix in mesoscopic scale at the resin rich prepreg interface.

End notched flexure (ENF) specimens (width: $B = 25$ mm, nominal thickness $2h = 3$ mm, length: 170 mm) were used for tests under static and fatigue loadings. Figure 1 shows the specimen and the loading apparatus. The distance between both supports, $2L$, was 100 mm, the length of the starter slit was 25 mm, and the crack length, a, is defined as the length between the crack tip and the support. Universal joints were used for the loading point and the supports in order to avoid uneven loading in the width direction of the specimen. Starter slits were introduced into

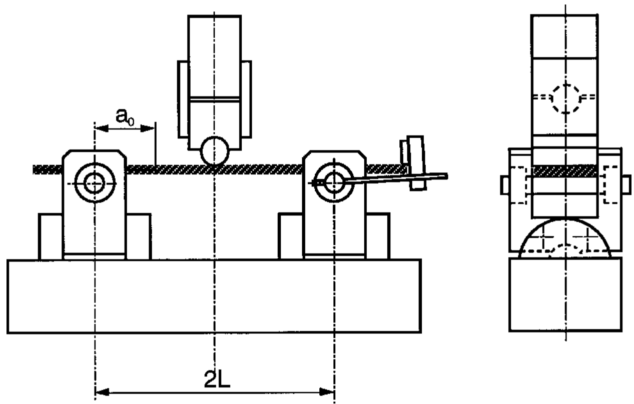

Figure 1. ENF specimen and loading apparatus.

the specimen by inserting 6 μm thick polyimide films (coated with a release agent) during molding at mid-thickness. Specimen edges were polished using abrasive papers and diamond paste to make crack-length measurement easier. For static tests, precracks were introduced under mode II fatigue loading. For fatigue tests, no precrack was introduced.

2.2. Calculation of fracture-mechanical parameters

Energy release rate, G, was calculated from the relation between the compliance, C, and the crack length, a, using the following equation:

$$G = P^2/(2B)\mathrm{d}C/\mathrm{d}a, \tag{1}$$

where P is the applied load. The relation between C and a is expressed by the following equation [6]:

$$E'BC(2h)^3 = \xi_0 + \xi_1 a^3, \tag{2}$$

where E' is the flexural modulus. Parameters ξ_0 and ξ_1 are computed from experimental calibration by using a least square program for each specimen.

2.3. Static and fatigue tests

Tests were carried out in a computer-controlled 10 kN servohydraulic testing machine (Shimadzu, EHF-ED-1) [6]. Static interlaminar fracture toughness tests were carried out by controlling the crack shear displacement (CSD, d) to stabilize the crack growth. The CSD rate was 0.03 mm/min based on JIS K7086-1993. The initial values of the fracture toughness, G_{IIc}, were calculated at the onset of nonlinearity of the initial load–displacement curve (NL), 5% offset point (5%), and the maximum load point ($P_{\max}$). The fracture toughness values during crack propagation are expressed as G_{IIR}.

Delamination fatigue crack growth tests were carried out with our original software [6, 7]. In each test, the stress ratio, R, of the minimum load to the maximum load was kept constant to be 0.5. The load-shedding rate, $1/G(\mathrm{d}G/\mathrm{d}a)$, was also controlled to be $-0.1\ \mathrm{mm}^{-1}$. The frequency of stress cycling was 10 Hz. The length of the crack was computed from equation (2). The tests were carried out in laboratory air.

3. EXPERIMENTAL RESULTS AND DISCUSSION

3.1. Static fracture toughness

The relation between the fracture toughness and the increment of the crack length is shown in Fig. 2. The fracture toughness values increased with the increment of the crack length, Δa, and then levelled off where Δa was larger than 3 mm for both laminates [6]. For the case of the non-treated CFRP, G_{IIc} at NL point was 610 $\mathrm{J/m^2}$, and that at $P_{\max}$ point (= 5% point) was 750 $\mathrm{J/m^2}$. G_{IIc} at NL point was 770 $\mathrm{J/m^2}$, and that at $P_{\max}$ point (= 5% point) was 1000 $\mathrm{J/m^2}$ for surface-treated CFRP. The average of the propagation values where Δa was larger than 3 mm, G_{IIs}, was 810 $\mathrm{J/m^2}$ and 1010 $\mathrm{J/m^2}$ for non-treated and surface-treated CFRP, respectively. The fracture toughness of the surface-treated CFRP was 25 to 30% higher than that of non-treated CFRP. This increase was almost the same for the initial values and the propagation values.

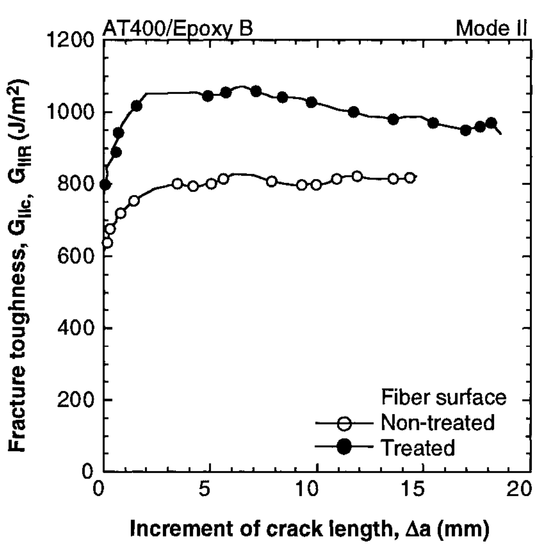

Figure 2. Effect of fiber surface treatment on mode II static crack growth resistance curves.

3.2. Fatigue crack growth behavior

Figure 3 compares the fatigue crack growth behavior between surface-treated and non-treated CFRP. The crack propagation rate, da/dN, is expressed as a power function of the maximum energy release rate, $G_{\mathrm{II\,max}}$, in the region where da/dN is larger than 10^{-9} m/cycle. Below this region, da/dN deviates to the lower rate from the power functions, and there exists the growth threshold for fatigue cracks. The figures associated with the straight lines indicate the exponents of the power functions. The threshold value, 120 J/m^2, was insensitive to the fiber surface treatment. In the higher rate region, da/dN for surface-treated CFRP was smaller than that for non-treated CFRP. The exponents of the power functions also showed the same tendency. Thus, the fatigue crack growth resistance of the surface-treated CFRP is higher with higher ductility.

3.3. Fractographic observation

Figures 4 and 5 show the scanning electron micrographs of the fracture surfaces under static and fatigue loadings for surface-treated and non-treated CFRP. For the case of static fracture toughness tests, interfacial fracture was dominant for the non-treated CFRP. Debonding of resin at the interface was often observed. On the other hand, the areal ratio of interfacial fracture and resin fracture was almost the same for the surface-treated CFRP. The fracture of resin brings hackles (microcracks perpendicular to the principal stress) and their plastic deformation. This is why the fracture toughness of the surface-treated CFRP was higher.

For fatigue fracture, interfacial fracture was about 60% at the high rate region, and about 40% near the threshold region for the non-treated CFRP. Large hackles

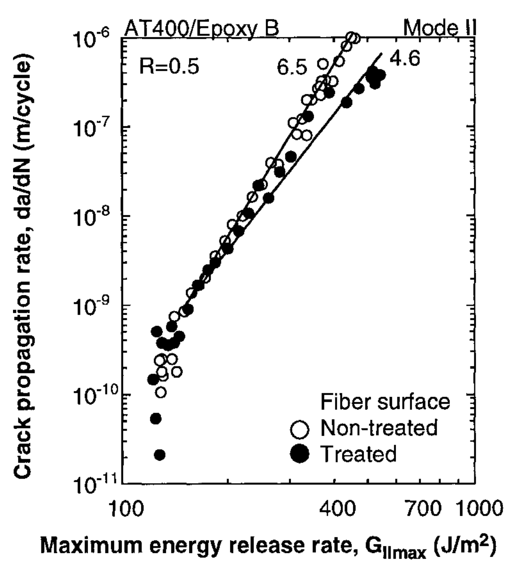

Figure 3. Effect of fiber surface treatment on mode II fatigue crack growth behavior.

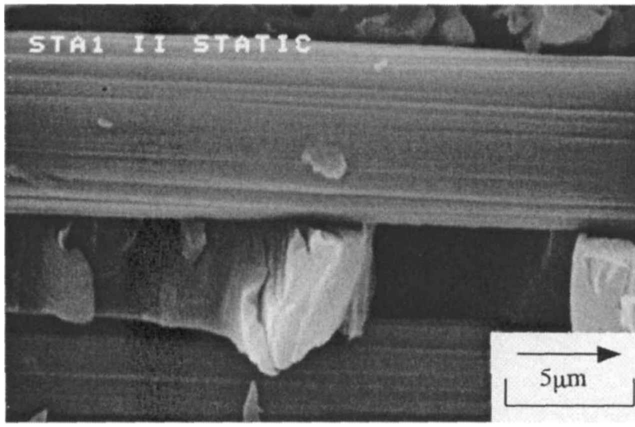

(a) Static fracture.

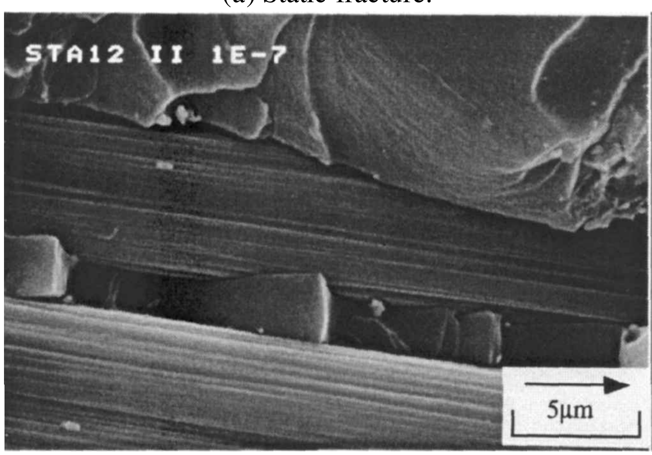

(b) Fatigue, $\mathrm{d}a/\mathrm{d}N = 1 \times 10^{-7}$ m/cycle.

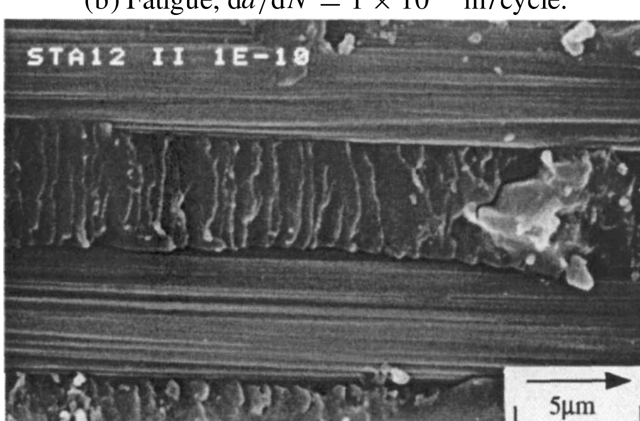

(c) Fatigue, $\mathrm{d}a/\mathrm{d}N = 1 \times 10^{-10}$ m/cycle.

Figure 4. Scanning electron micrographs of fracture surfaces for non-treated CFRP.

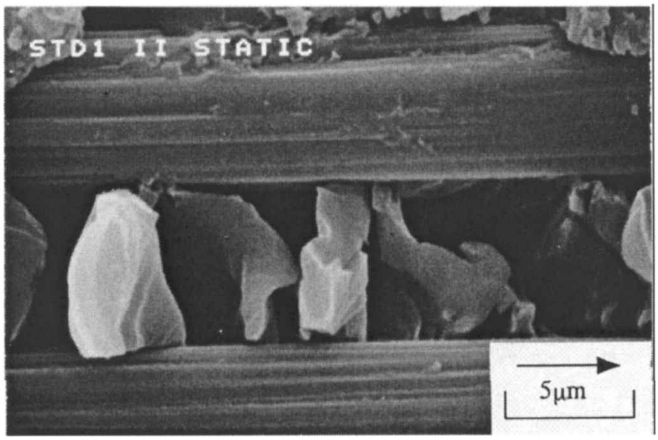

(a) Static fracture.

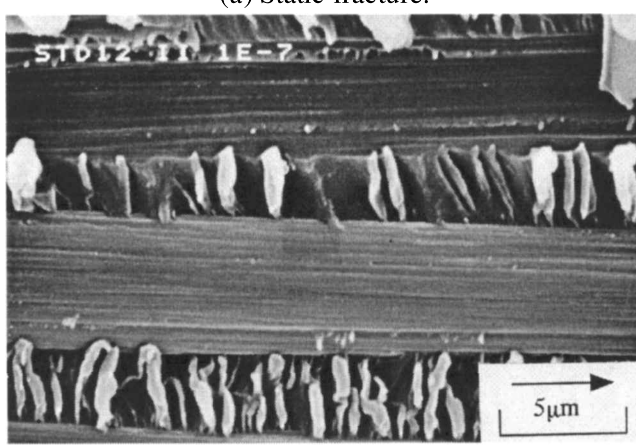

(b) Fatigue, $da/dN = 1 \times 10^{-7}$ m/cycle.

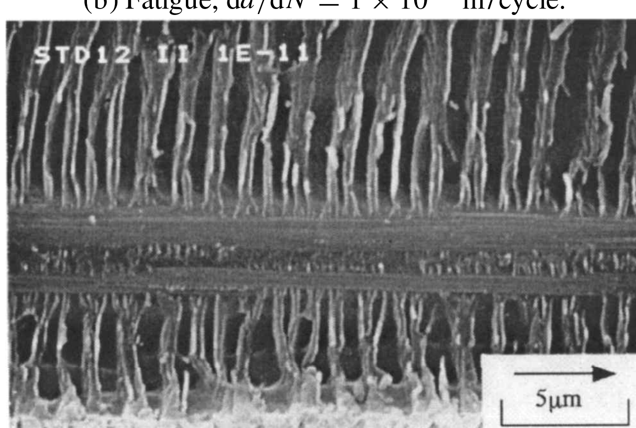

(c) Fatigue, $da/dN = 1 \times 10^{-10}$ m/cycle.

Figure 5. Scanning electron micrographs of fracture surfaces for surface-treated CFRP.

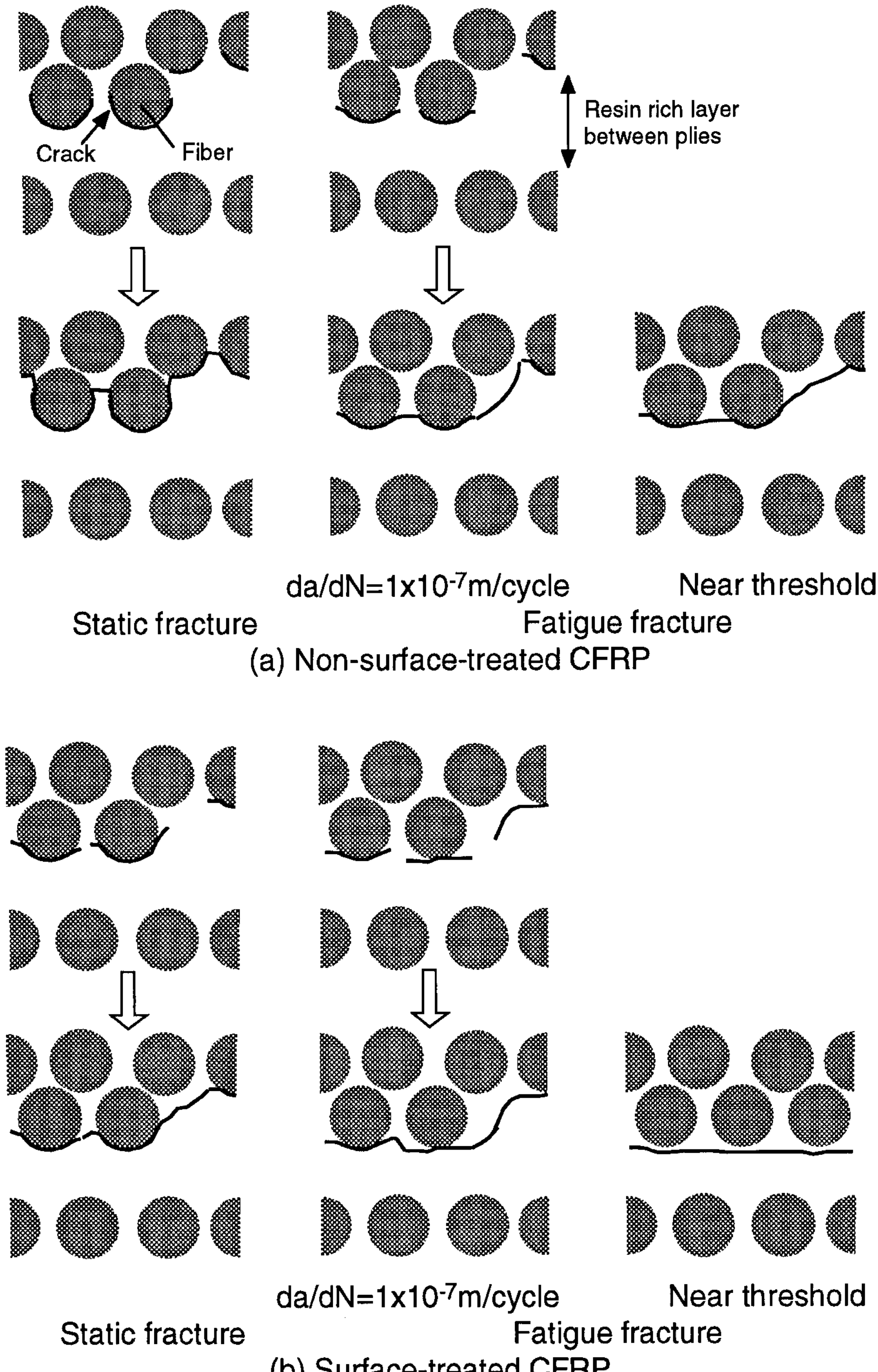

Figure 6. Schematic drawing of fracture process in transverse section of CFRP with and without fiber surface treament.

Table 1.
Summary of features of fracture surfaces, observed using scanning electron microscopy

	Non-treated CFR			Treated CFRP		
	Static fracture	Fatigue fracture		Static fracture	Fatigue fracture	
		1×10^{-7} m/cycle	1×10^{-10} m/cycle		1×10^{-7} m/cycle	1×10^{-10} m/cycle
Main fracture path	Interface	Interface	Resin	Interface/Resin	Resin	Resin
Areal ratio of interfacial fracture	80%	60%	40%	50%	30%	10%
Interval of hackles	10 μm	10 μm	<1 μm	10 μm	1–5 μm	<1 μm
Microscopic delamination between fiber and matrix	○	○	○	×	×	×
Plastic deformation	○	×	—	○	○	—

of the interval of 10 μm were observed at the high rate region. For the case of the surface-treated CFRP, 70% of the fracture surface was resin fracture at the high rate region, and the areal ratio increased to 90% near the threshold region. Only small hackles of the interval of 1 to 5 μm were observed at the high rate region. Near the threshold, the resin part was rather flat, and composed of small hackle-like patterns of an interval of less than 1 μm without respect to the surface treatment. The main fracture mechanism near the threshold region was controlled by the matrix resin for both surface-treated and non-treated CFRP, and this was well correlated to the fact that the threshold value was insensitive to the fiber surface treatment. The results of the fractographic observation was summarized in Table 1.

Observation of transverse section of the specimen near the crack tip was also carried out in order to clarify whether interfacial fracture or resin fracture first occurred at the crack tip under fatigue loading. While the interfacial fracture occurred prior to the matrix fracture for the non-treated CFRP in the higher growth rate region, the matrix fracture occurred in advance for the surface-treated CFRP. This difference was schematically shown in Fig. 6. This difference of the fracture mechanism is responsible for the higher $\mathrm{d}a/\mathrm{d}N$ and the larger exponent of the power function of the non-treated CFRP.

4. CONCLUSION

Fiber surface treatment had different effect on mode II interlaminar fracture under static and fatigue loadings. Interlaminar fracture toughness of surface-treated CFRP was about 25 to 30% higher than that of non-treated CFRP. On the other hand, the growth threshold of the delamination fatigue crack was insensitive to the fiber surface treatment. This difference of the effect of the surface treatment was explained by the difference of the fracture path in mesoscopic scale based on the microscopic observation.

REFERENCES

1. L. M. Manocha, Role of fiber surface–matrix combination in carbon fiber reinforced epoxy, *J. Mater. Sci.* **17**, 3039–3044 (1982).
2. M. S. Madhukar and L. T. Drzal, Fiber–matrix adhesion and its effect on composite mechanical properties, *J. Compos. Mater.* **25**, 932–957 (1991).
3. N. Tsujioka, Z. Maekawa, H. Hamada and M. Hojo, Effect of surface oxidation and sizing treatment of carbon fiber on interfacial adhesion, *J. Soc. Mater. Sci. Japan* **46**, 163–169 (1997).
4. M. Hojo, S. Ochiai, N. Tsujioka, M. Kotaki, H. Hamada and Z. Mekawa, High technology composites in modern applications, in: *Proc. COMP '95*, pp. 30–36. Univ. of Patras, Greece (1995).
5. Y. Nakanishi and N. Ikuta, Interphase of FRP and its chemical control, *J. Soc. Mater. Sci. Japan* **45**, 1307–1315 (1996).
6. M. Hojo, S. Matsuda, T. Higuchi and S. Ochiai, Fracture mechanism for Mode II propagation of delamination fatigue cracks in CF/PEEK laminates, *J. Soc. Mater. Sci. Japan* **46**, 366–373 (1997).
7. M. Hojo, S. Ochiai, C.-G. Gustafson and K. Tanaka, Effect of matrix resin on delamination fatigue crack growth in CFRP laminates, *Engineering Fracture Mechanics* **49**, 35–47 (1994).